Cell PRESS
Neuron
Article

Polycomb Limits the Neurogenic Competence of Neural Precursor Cells to Promote Astrogenic Fate Transition

Yusuke Hirabayashi,[1] Nao Suzki,[1] Masafumi Tsuboi,[1] Takaho A. Endo,[2] Tetsuro Toyoda,[2] Jun Shinga,[3] Haruhiko Koseki,[3] Miguel Vidal,[3,4] and Yukiko Gotoh[1,*]
[1]Institute of Molecular and Cellular Biosciences, University of Tokyo, Tokyo, Japan
[2]RIKEN Genomic Sciences Center
[3]RIKEN Center for Allergy and Immunology
Kanagawa, Japan
[4]Centro de Investigaciones Biológicas, Consejo Superior de Investigaciones Científicas, Madrid, Spain
*Correspondence: ygotoh@iam.u-tokyo.ac.jp
DOI 10.1016/j.neuron.2009.08.021

SUMMARY

During neocortical development, neural precursor cells (NPCs, or neural stem cells) produce neurons first and astrocytes later. Although the timing of the fate switch from neurogenic to astrogenic is critical for determining the number of neurons, the mechanisms are not fully understood. Here, we show that the polycomb group complex (PcG) restricts neurogenic competence of NPCs and promotes the transition of NPC fate from neurogenic to astrogenic. Inactivation of PcG by knockout of the *Ring1B* or *Ezh2* gene or *Eed* knockdown prolonged the neurogenic phase of NPCs and delayed the onset of the astrogenic phase. Moreover, PcG was found to repress the promoter of the proneural gene *neurogenin1* in a developmental-stage-dependent manner. These results demonstrate a role of PcG: the temporal regulation of NPC fate.

INTRODUCTION

The mechanism regulating the timing of stem cell fate switching is crucial for understanding tissue development. Neurons and astrocytes in the neocortex are derived from common multipotent NPCs which sequentially pass through phases of expansion, neurogenesis and astrogenesis (Hirabayashi and Gotoh, 2005; Miller and Gauthier, 2007). The production of neurons before astrocytes allows the initial establishment of a neuronal network and subsequent integration of astrocytes into the network. The timing of the neurogenic-to-astrogenic fate switch is critical for brain development, in particular because the length of the neurogenic phase is a key parameter in determining the number of neurons in each brain region.

NPC fate is regulated by both extracellular signals and cell-intrinsic programs (Desai and McConnell, 2000). The extracellular signals, including ciliary neurotrophic factor (CNTF), leukemia inhibitory factor (LIF), and cardiotrophin-1 (CT-1), activate the JAK-STAT pathway, which plays a pivotal role in the promotion of astrocytic differentiation (Barnabe-Heider et al., 2005; Bonni et al., 1997; He et al., 2005; Johe et al., 1996; Rajan and McKay, 1998). The bone morphogenetic protein (BMP) and Notch pathways also interact with the JAK-STAT pathway to promote astrocytic differentiation (Gaiano and Fishell, 2002; Kamakura et al., 2004; Nakashima et al., 1999). However, some ligands that activate the JAK-STAT pathway are expressed during the neurogenic phase when astrocytic genes are silent (Molne et al., 2000). At least three mechanisms have been proposed to account for the suppression of astrocytic genes during the neurogenic phase. First, STAT responsive elements at the astrocytic gene loci are inaccessible for STAT proteins during the neurogenic phase due to DNA or histone H3K9 methylation (Fan et al., 2005; Song and Ghosh, 2004; Takizawa et al., 2001). Second, astrocytic genes are inactivated by erbB4-NCoR signaling during the neurogenic phase (Sardi et al., 2006). And third, STAT proteins are inactivated by the proneural basic helix-loop-helix (bHLH) transcription factors present during the neurogenic phase.

Genetic and molecular evidence has established the essential roles of proneural bHLH proteins in suppressing astrocytic fate (Guillemot, 2007), such that deletion of bHLH genes causes precocious astrocyte differentiation and loss of the neuronal fate (Nieto et al., 2001; Tomita et al., 2000). Two such bHLH transcription factors, Neurogenin (Ngn) 1 and Ngn2, are expressed solely during the neurogenic, not in the astrocytic, phase of neocortical development (Sun et al., 2001, and references therein). Ngn1 expression in vitro and in vivo can suppress astrocytic differentiation of NPCs in part because Ngn1 sequesters the p300/CBP-Smad1 complex from STAT3, which leads to STAT3 inactivation/dephosphorylation (Cai et al., 2000; Guillemot, 2007; Sun et al., 2001). Since STAT3 activation is necessary for astrogenesis to occur (He et al., 2005), the expression of bHLH proteins can suppress astrogenesis even when astrocytic genes are released from erbB4-NCoR signaling and demethylated. Turning off the bHLH proteins is therefore a critical event for the onset of astrocyte differentiation.

The regulation of proneural bHLH genes, primarily Ngn1 and Ngn2 in the neocortex, is thus key for understanding phase

transition in NPCs (Guillemot, 2007). Wnt signaling has been shown to induce the expression of *ngn1* and *ngn2* and promote neocortical neuronal differentiation (Hirabayashi et al., 2004; Israsena et al., 2004). However, Wnt ligands continue to be expressed during the astrogenic phase (Shimogori et al., 2004), suggesting that their effect on Ngn1 and Ngn2 is somehow blocked.

The neurogenic-to-astrogenic fate switch can be observed even within clones of single NPCs in culture, suggesting that cell-intrinsic programs also play essential roles (Naka et al., 2008; Qian et al., 2000). The intrinsic mechanisms may change the responsiveness of NPCs to fate-regulating extracellular signals and thus control the timing of the fate switch. For instance, intrinsic mechanisms may suppress Wnt induction of Ngn expression during the gliogenic phase and derepress STAT3 so that NPCs can respond to astrocyte-promoting cytokines.

It has become increasingly clear in recent years that epigenetic events control responsiveness of each cell to extrinsic signals and govern cell fate decisions. Polycomb group (PcG) proteins have emerged as central players in these epigenetic programming events. PcG proteins are transcription repressors that function by modulating chromatin structure (Schwartz and Pirrotta, 2007). They reside in two main complexes referred to as polycomb repressive complexes 1 and 2 (PRC1 and PRC2). PRC2 contains Eed, Suz12, and the methyltransferase Ezh1 or Ezh2 that catalyzes histone H3 lysine 27 trimethylation (H3K27me3) (Cao and Zhang, 2004; Shen et al., 2008). This histone modification then provides a platform to recruit PRC1, which contains the ubiquitin ligase Ring1 (Ring1A or Ring1B), an essential component for PcG-mediated repression (de Napoles et al., 2004). Although PcG proteins have been demonstrated to play critical roles for the maintenance of ES cells as well as adult stem cell populations such as hematopoietic and neural stem cells (Spivakov and Fisher, 2007; Valk-Lingbeek et al., 2004), their roles in multipotent progenitors during tissue development have largely remained unclear.

In this study, we show that the PcG proteins epigenetically suppress the *ngn1* locus during the astrogenic phase and thus trigger the neurogenic-to-astrogenic fate switching of NPCs and regulate the duration of the neurogenic phase in the developing neocortex.

RESULTS

Temporal Restriction of Neurogenic Competence in the Neocortical NPCs

Previously, we and others showed that the canonical Wnt pathway induces expression of *ngn1* and *ngn2* and functions instructively to promote neuronal differentiation of neocortical NPCs (Guillemot, 2007; Hirabayashi and Gotoh, 2005; Hirabayashi et al., 2004; Israsena et al., 2004; Zhou et al., 2006). It was puzzling, however, that Wnt ligands continue to be expressed during the astrogenic phase (Shimogori et al., 2004). We examined whether the response of NPCs to Wnt signaling is dependent on the developmental stage using in vitro culture methods (Qian et al., 2000). Neuroepithelial cells isolated from E11.5 neocortex were cultured for 3, 6, and 9 days in vitro (DIV) as a suspension in the presence of fibroblast growth factor (FGF) 2 and epidermal growth factor (EGF) and subsequently plated onto poly-D-lysine-coated dishes. Cells were infected with either control retrovirus or retrovirus encoding a stabilized β-catenin (S33Yβ-catenin), which constitutively activates the canonical Wnt pathway (Korinek et al., 1997). Under these conditions, more than 99% of infected (GFP-positive) cells are nestin-positive undifferentiated NPCs, and 3 and 9 DIV cultures correspond to the neurogenic and astrogenic phases, respectively (Hirabayashi and Gotoh, 2005; Qian et al., 2000). Three days after infection of 3 DIV cultures with S33Yβ-catenin virus, the proportion of cells positive for the neuronal marker β3-tubulin (TuJ1) markedly increased (Figures 1A and 1B). In contrast, expression of S33Yβ-catenin had less of an effect on neuronal differentiation in 9 DIV cultures (Figures 1A and 1B). Expression of S33Yβ-catenin also had less of an effect on neuronal differentiation of 3 DIV culture isolated from E17.5 neocortex compared to that of 3 DIV culture isolated from E11.5 neocortex (Figure 1B). Therefore, the effects of S33Yβ-catenin on neuronal differentiation appear to decrease with age. As a control, enforced expression of *ngn1* in NPCs of any age did induce neuronal differentiation (Figures 1A and 1B). Consistent with this observation, the effect of S33Yβ-catenin on increasing the amounts of *ngn1* and *ngn2* mRNAs were also reduced in 9 DIV NPCs compared to 3 DIV NPCs (Figures 1C and S3A). These results suggest that NPCs lose their capacity to differentiate into neurons in response to the canonical Wnt pathway during late stages of development. In addition, they imply that a step between β-catenin activation and *ngn1* expression is blocked in the late/astrogenic stage of development.

We considered the possibility that this blockade was due to the absence of components of the β-catenin/TCF transcriptional complex at late stages. However, we found that S33Yβ-catenin stimulates expression of SuperTOP-FLASH, a luciferase reporter gene construct expressed under the control of TCF-responsive elements (Kaykas et al., 2004), in both E11.5 + 3 DIV and 12 DIV cultures (Figure 1D). Moreover, treatment of cultures for 2 hr with the GSK3 inhibitor SB216763, which activates the canonical Wnt pathway (Cohen and Goedert, 2004), induced *Axin2*, an immediate-early gene in the canonical Wnt pathway (Aulehla et al., 2003), to a similar extent in both E11.5 + 3 DIV and 9 DIV cultures (Figure S1). Therefore, β-catenin appears to be able to form an active transcriptional complex with TCF even in late-stage cells.

Temporal Change of the Chromatin State at Neurogenin Promoters

We tested whether the epigenetic chromatin state of *ngn* gene loci changes during development. We first examined the DNA methylation status of the *ngn1* promoter by the bisulfite direct sequence method (Clark et al., 1994) but found that the *ngn1* promoter was barely methylated in either E11.5 + 3 DIV or 9 DIV cultures (Figure S2). We next investigated posttranslational modification of histone H3 bound to the *ngn* promoters using chromatin immunoprecipitation (ChIP). Histone H3 acetylation at Lys9 and Lys14 (H3K9K14ac) or trimethylation at Lys9 and Lys27 (H3K9me3 and H3K27me3) in general correlates with open or closed chromatin state, respectively (Berger, 2002; Cao and Zhang, 2004). H3K9K14ac was enriched at the proximal

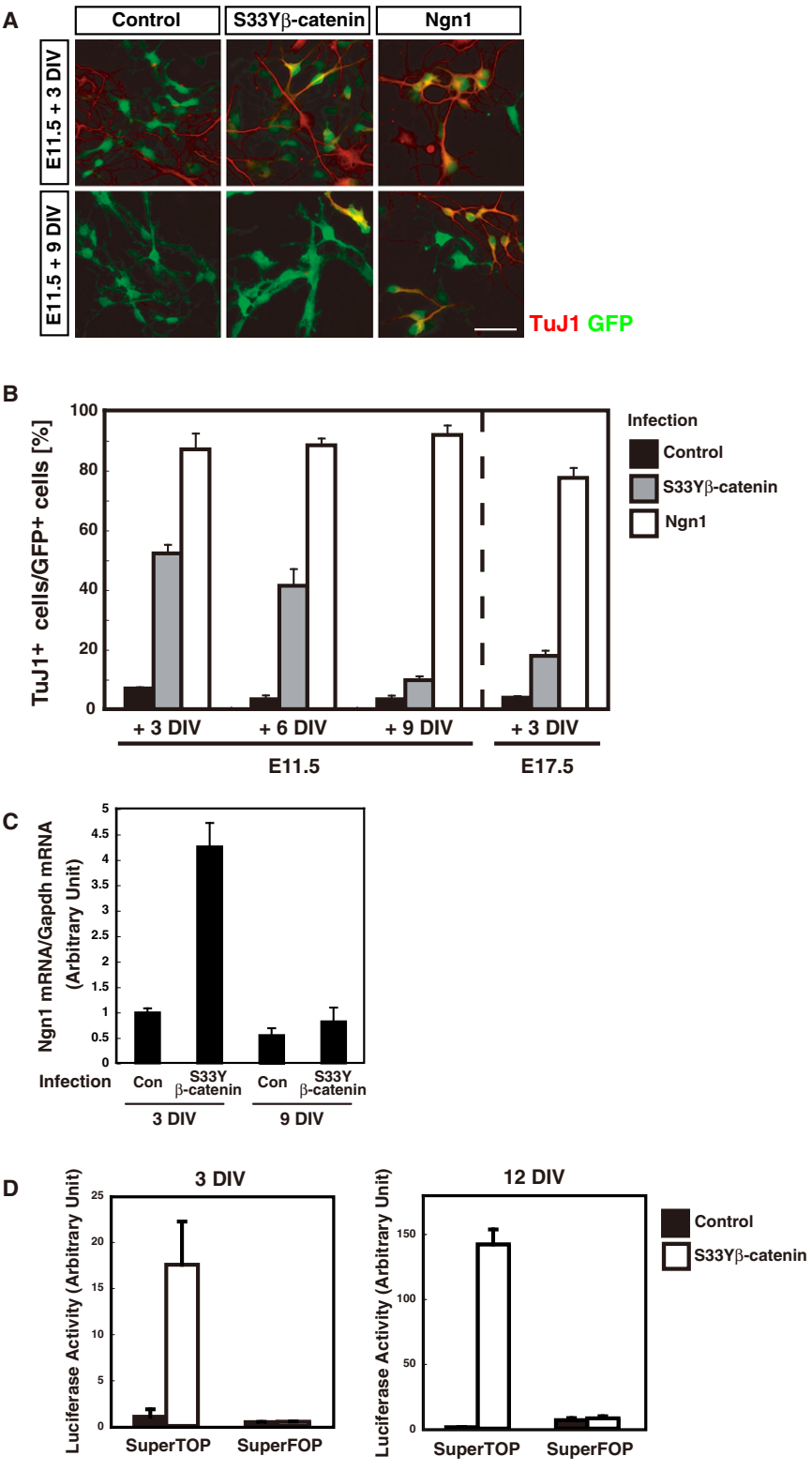

Figure 1. NPCs Lose Their Capacity to Differentiate into Neurons in Response to the Canonical Wnt Pathway at Late Stages of Development

NPCs isolated from E11.5 were cultured for 3, 6, or 9 DIV, and E17.5 cells were cultured for 3 DIV. Next the cells were infected with a retrovirus encoding GFP alone (control), GFP together with S33Yβ-catenin, or Ngn1 and incubated for an additional 3 days with FGF2.

(A) Anti-GFP (green) and TuJ1 (red) immunofluorescence are shown for typical fields in control, S33Yβ-catenin, or Ngn1-expressing cells.

(B) The percentage of $TuJ1^+$ cells among GFP^+ cells was determined. Data are means + SEM of values from four samples.

(C) E11.5 NPCs cultured for the indicated periods were infected with a retrovirus encoding GFP alone (control) or GFP together with S33Yβ-catenin and incubated for 3 days with FGF2 and subsequently for 3 hr without FGF2. The amount of *ngn1* mRNA was determined at the end of these treatments by quantitative PCR. Data are means + SEM of values from three samples.

(D) E11.5 NPCs cultured for the indicated periods were transfected with pMX-S33Yβ-catenin (open bars) or empty vector (filled bars), together with Super TOP-FLASH or Super FOP-FLASH (a negative control reporter plasmid with a mutated TCF binding site) for 20 hr. Data are means + SEM of values from three samples. Scale bar, 20 μm.

(around TATA box) region of the *ngn1* and *ngn2* promoters compared to the intergenic region in E11.5 + 3 DIV cultures, but its levels were reduced gradually in the late-stage cultures (Figures 2A–2C and S3B). Furthermore, the levels of H3K27me3 at the *ngn1* and *ngn2* promoters increased gradually in late-stage cultures (Figures 3A and S3C), whereas the levels of H3K9me3 and H3K9me2 at these promoters remained low in both early and late cultures (data not shown). Developmental increases in the levels of H3K27me3 at the *ngn1* and *ngn2* promoters were also found in NPCs isolated from E14 and E17 neocortices (Figures S3D and S5A). These results suggest that the chromatin state of the *ngn* promoters gradually becomes closed over time during development, and *ngn* genes are thus transcribed less in the late stages. Consistent with this notion, the levels of RNA polymerase II associated with the *ngn* promoters were reduced in the late cultures (Figures 2D, S3E, and S5B).

We then asked whether stage-dependent changes in histone deacetylation affected *ngn* expression by treating NPCs with the histone deacetylases (HDAC) inhibitor valproic acid (VPA) (Gottlicher et al., 2001). VPA treatment for 16 hr increased the levels of H3K9K14ac at the *ngn1* promoter (Figure 2E)

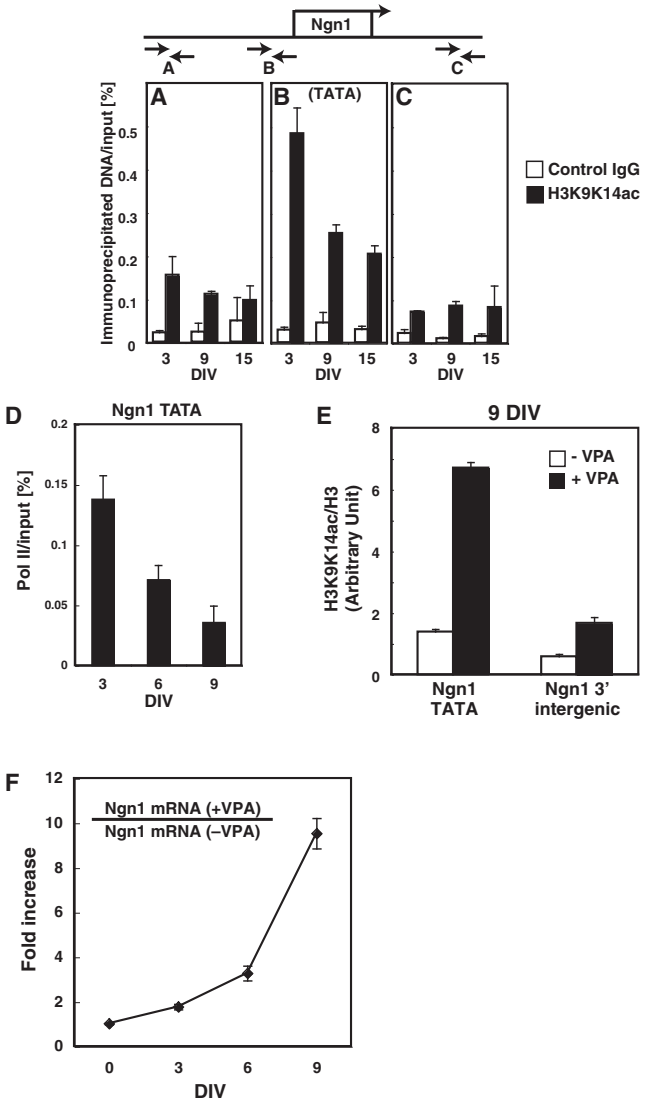

Figure 2. Decreases in the Level of H3K9K14 Acetylation at the *ngn1* Promoter Result in the Repression of *ngn1* mRNA Expression

Chromatin complex was immunoprecipitated from E11.5 neocortical NPCs cultured for 3, 9, or 15 DIV with anti-H3K9K14ac (A–C) or anti-RNA polymerase II (D). The immunoprecipitates were subjected to PCR amplification of −1299 to −976 (TCF site [A], −45 to +39 [TATA box, B and D], and +5170 to +5274 [intergenic, C] base pairs from the transcription start site of *ngn1* gene. (E) The level of acetylation at the *ngn1* promoter in VPA-treated (filled bars) or untreated cells (open bars) was determined by ChIP. (F) The fold change of *ngn1* mRNA amounts caused by VPA treatment at indicated culture periods was measured (see Figure S4A for absolute values). Data are means + SEM of values from three samples.

and significantly increased *ngn1* expression (Figures 2F and S4A) in E11.5 + 9 DIV culture. In contrast, VPA treatment caused only a small increase in *ngn1* expression in E11.5 + 0 or 3 DIV cultures (Figures 2F and S4A). This suggests that histone deacetylation suppresses the expression of *ngn1* in late-stage cultures.

PRC1 Suppresses *ngn1* Expression in the Late Stage of Neocortical Development

We then examined the role of H3K27me3 in *ngn* expression. Trimethylation of H3K27 is catalyzed by PRC2, which includes Eed, Suz12, and the histone methyltransferase Ezh2 (or Ezh1) (Cao and Zhang, 2004; Shen et al., 2008). This modification is recognized by PRC1, which induces a closed chromatin state (Schwartz and Pirrotta, 2007). We inactivated PRC1 by conditional deletion of an essential component, the ubiquitin ligase *Ring1B* (de Napoles et al., 2004; Voncken et al., 2003). Neocortical NPCs were isolated from E12.5 mice containing both *Ring1B* alleles flanked by the loxP sequences (*Ring1B*$^{f/f}$) and a transgene expressing tamoxifen-dependent Cre recombinase under the control of the endogenous ROSA26 promoter (ROSA26::ERT2-Cre) (Cales et al., 2007; Endoh et al., 2008). Treatment of NPCs isolated from the *Ring1B*$^{f/f}$;ERT2-Cre mice with 4-hydroxy-tamoxifen (4-OHT) effectively reduced Ring1B expression (Figure 3B). Following treatment, the levels of *ngn1* mRNA in the 9 DIV cultures markedly increased (~8-fold), whereas those in the 3 DIV cultures exhibited a much smaller increase (~1.6-fold) (Figures 3C and S4B). This indicates that the *Ring1B* gene contributes to the suppression of *ngn1* expression in the late stages of neocortical development. Inhibition of HDAC further enhanced *ngn1* expression induced by the loss of *Ring1B* gene to levels comparable with those in the early stage (3 DIV) cultures (Figures 3D and S4B). This suggests that HDACs and PRC1 function cooperatively in the suppression of *ngn1* at late stages of neocortical development. Consistent with this notion, expression of S33Yβ-catenin enhanced the levels of *ngn1* mRNA even in late stage (9 DIV) cultures when *Ring1B* was deleted (Figure 3E). On the other hand, the levels of *ngn2* mRNA were only moderately enhanced or even reduced by the loss of *Ring1B* gene and by inhibition of HDACs, with or without activation of Wnt signaling (Figures S3F, S3G, S3H, and Table S1). Therefore, additional mechanisms might also contribute to the suppression of *ngn2* expression in the late stage of neocortical development.

Next, we examined *ngn1* expression in vivo during neocortical development. Immunohistochemistry revealed that Ngn1 was highly expressed at E14.5 in the ventricular zone (VZ) of neocortex, but its expression gradually declined until E17.5, when only a small number of cells at the neocortical VZ were found to express Ngn1 protein (Figures 3H and S6A). However, when the *Ring1B* gene was deleted in *Ring1B*$^{f/f}$;ERT2-Cre mice by injecting tamoxifen intraperitoneally into pregnant mice at 12.5 days postcoitum (dpc) (Figure 3G), the number of Ngn1-expressing cells in the VZ increased at E17.0 or E17.5 to levels comparable with those in the late neurogenic phase (e.g., E16.5, see Figure S6A) (Figures 3H–3J). *Ring1B* deletion did not increase the number of Ngn1-expressing cells at early stages of the neurogenic phase (e.g., E14.5, Figure S6B). Increase in Ngn1 protein by *Ring1B* deletion in the neocortex at E17.5 was confirmed by western blot analysis (Figures 3L and 3M). Quantitative RT-PCR analysis also indicated that the amounts of *ngn1* mRNA, but not those of *ngn2* mRNA, were significantly greater in the lysates of *Ring1B*-deficient cortices compared to those of control ones prepared at E18.5 (Figures 3K and S3I). These results demonstrate an in vivo role for

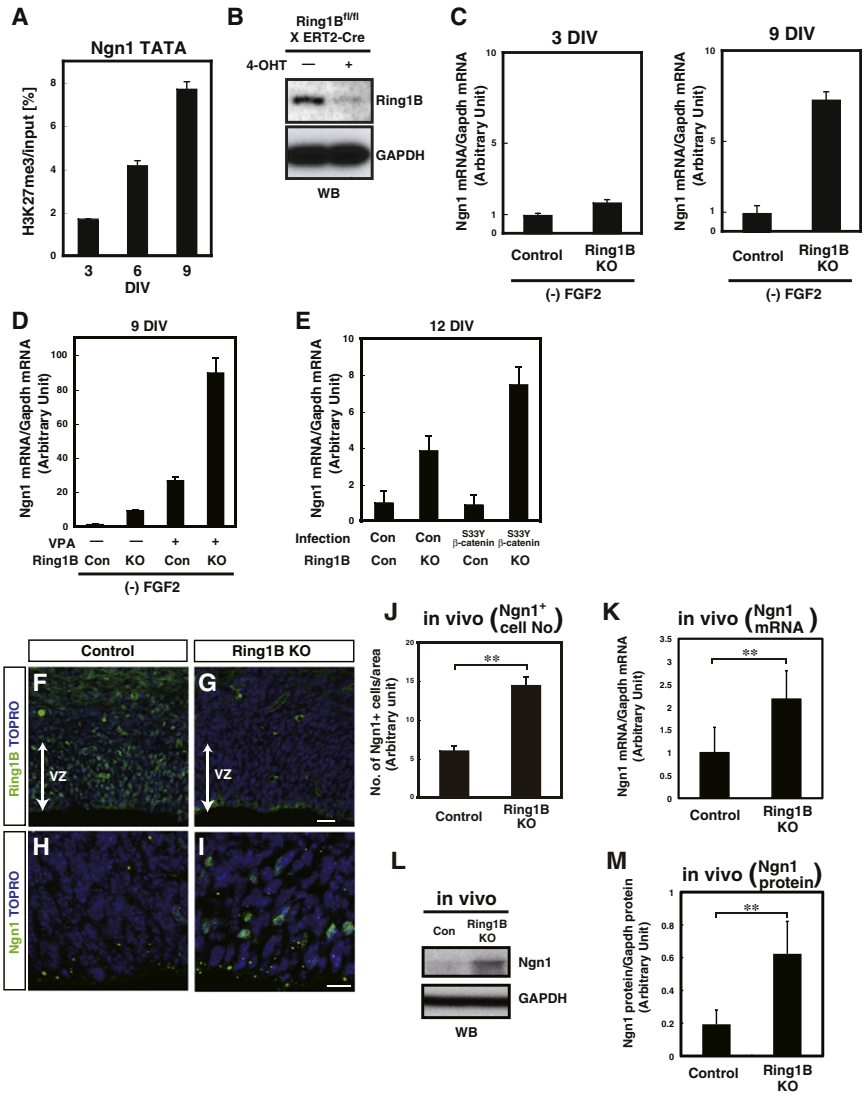

Figure 3. Ring1B/PRC1 Suppresses *ngn1* Expression at Late Stages of Neocortical Development

(A) Abundance of H3K27 trimethylation at the *ngn1* promoter (TATA box) was assessed by ChIP and quantitative PCR from E11.5 neocortical NPCs cultured for 3, 6, or 9 DIV.

(B and C) NPCs isolated from E12.5 *Ring1B*$^{f/f}$; ERT2-Cre mice were cultured for 0 or 6 DIV and cultured for an additional 3 DIV with 4-OHT (KO) or EtOH (Con). After 3 hr of FGF2 deprivation, the amount of *ngn1* mRNA was determined at the end of these treatments by quantitative PCR (see Figure S4B for absolute values). Data are means + SEM of values from three samples. Cell lysates at 3 DIV were subjected to western blotting (WB) using the antibodies indicated (B).

(D and E) The cells were further cultured in the absence of 4-OHT, with or without VPA for 1 day and, subsequently, without FGF2 for 2 hr (D). NPCs isolated from E12.5 *Ring1B*$^{f/f}$;ERT2-Cre mice were cultured for 6 DIV, infected with a retrovirus encoding GFP (Con) or GFP together with S33Y β-catenin and cultured for an additional 3 DIV with 4-OHT (KO) or EtOH (Con) (E). The amount of *ngn1* mRNA was then determined. Data are means + SEM of values from three samples.

(F–M) Tamoxifen was introduced into control (*Ring1B*$^{f/f}$) mice (F and H) or *Ring1B*$^{f/f}$;ERT2-Cre mice (G and I) at E12.5. At E17.0, embryos were fixed and subjected to immunohistochemistry using the antibodies against Ring1B (F and G) or Ngn1 (H and I). Nuclei were counterstained with Topro-3. Note that the number of Ngn1$^+$ cells in the neocortical ventricular zone (VZ) increased by *Ring1B* deletion. Scale bars, (G) 20 μm, (I) 10 μm.

(J) Quantification of Ngn1$^+$ cells at E17.5. Data are the mean + SEM of values for ten (control) or nine (KO) areas of corresponding sections from each embryo analyzed. In (K)–(M), neocortical lysates were prepared at E18.5 (K) or E17.5 (L, M), and the amounts of *ngn1* mRNA (K) or protein (L and M) were determined. (K) Data are the mean + SEM of values for four control cortices and 12 KO cortices analyzed. (M) Data are the mean + SD of values for five control cortices and three KO cortices analyzed by western blotting (L). *$p < 0.05$; **$p < 0.005$.

Ring1B in the suppression of Ngn1 at the end of the neurogenic phase.

PRC1 Restricts Neurogenic Competence at Late Stages of Neocortical Development

The next key question is whether *Ring1B* is necessary for the suppression of the neurogenic fate at late stages of development. In the absence of neurogenic signals, deletion of *Ring1B* from NPCs isolated from *Ring1B*$^{f/f}$;ERT2-Cre mice by 4-OHT treatment had little effect on neuronal differentiation at either E11.5 + 3 DIV or 9 DIV (Figures 4A and 4B), suggesting that the loss of *Ring1B* on its own does not result in neurogenesis. By contrast, loss of *Ring1B* gene significantly enhanced neuronal differentiation induced by S33Yβ-catenin expression at 9 DIV, but it had less effect at 3 DIV (Figure 4A). Similarly, deletion of *Ring1B* by treatment with 4-OHT enhanced the S33Yβ-catenin-induced neuronal differentiation of NPCs from E17.5 *Ring1B*$^{f/f}$;ERT2-Cre mice cultured for 3 DIV (data not shown). The loss of *Ring1B* also significantly enhanced neuronal differentiation induced by growth factor deprivation at E11.5 + 9 DIV (Figure 4B). These results suggest that PRC1 contributes to the suppression of neurogenic "competence" during late stages of NPC culture.

The deletion of *Ring1B* from E11.5 + 9 DIV NPC cultures isolated from *Ring1B*$^{f/f}$;ERT2-Cre mice by 4-OHT treatment had little effect on the rate of cell proliferation detected by BrdU incorporation (Figure 4C) or cell death detected by cleaved caspase-3 (less than 3% of infected cells). Furthermore, *Ring1B* deletion markedly increased the proportion of neuron-only and neuron-containing clones at the expense of nonneuronal clones

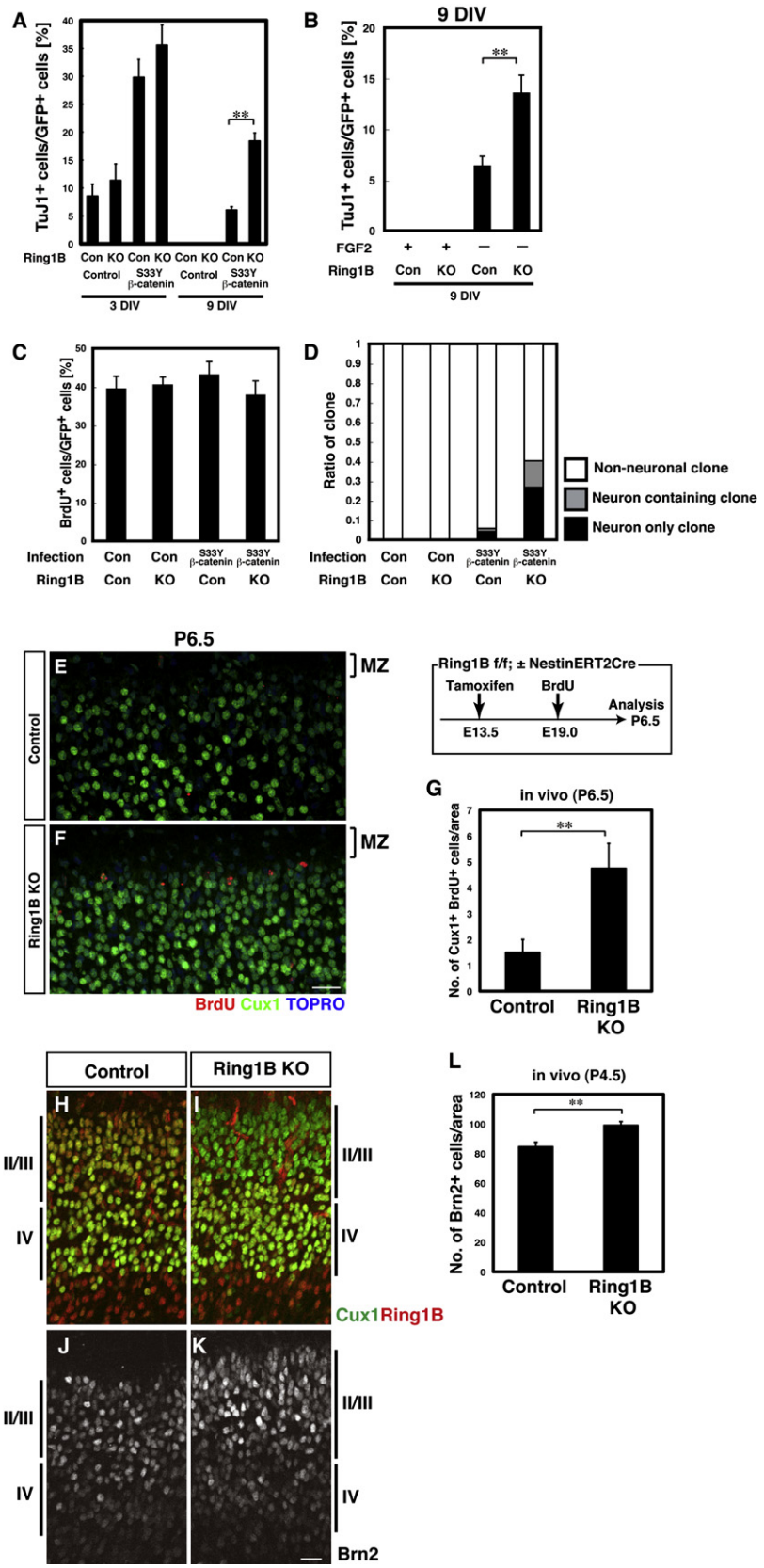

Figure 4. Ring1B/PRC1 Is Necessary for the Termination of Neurogenesis in the Neocortex

(A and B) E12.5 *Ring1B*$^{f/f}$;ERT2-Cre NPCs were cultured for 0 or 6 DIV and then treated with 4-OHT (KO) or EtOH (Con) for an additional 3 DIV. Cells were then plated and infected with a retrovirus encoding GFP (Control) or GFP together with S33Yβ-catenin in the presence of FGF2 (A) or incubated with or without FGF2 (B). After 2 days, the percentage of TuJ1$^+$ cells among GFP$^+$ cells was determined. Data are means + SEM of values from three samples.

(C) Cells at 9 DIV were incubated with BrdU for 2 hr at the end of the treatments in (A). The percentage of BrdU$^+$ cells among GFP$^+$ cells was determined. Data are means + SEM of values from three samples.

(D) A clonal analysis of (A). E12.5 *Ring1B*$^{f/f}$;ERT2-Cre NPCs were cultured for 9 DIV and then treated with 4-OHT (KO) or EtOH (Con) for an additional 3 DIV. Cells were infected with a retrovirus encoding GFP (Control) or GFP together with S33Yβ-catenin at a low titer. After incubation in the presence of FGF2 for 2 days, cells in each clone were stained with TuJ1 antibody, and the clones were classified as containing either only TuJ1$^+$ cells (neuron-only clone), both TuJ1$^+$ and TuJ1$^-$ cells (neuron-containing clone), or only TuJ1$^-$ cells (nonneuronal clone).

(E–L) *Ring1B*$^{f/f}$;NestinCreERT2 mice or control (*Ring1B*$^{f/f}$) mice were administrated with tamoxifen at E13.5 (E–G) or E16.0 (H–L) and BrdU at E19.0 (E–G). The pups were fixed at P6.5 (E–G) or P4.5 (H–L) and subjected to immunohistochemistry using the antibodies indicated. Coronal sections of primary sensory area in the neocortex are shown. In (G), neuronal differentiation was determined by examining cells positive for both BrdU and the upper layer neuronal marker Cux1 (Nieto et al., 2004) located in the upper layers. In (L), the numbers of Brn2-positive cells located in the upper layers were determined. Data are the mean + SD of values for three control and four KO mice (E–G) and the mean + SEM of values for 16 corresponding areas each from two control mice or five knockout mice (L). MZ, marginal zone ; II/III, layer II/III ; IV, layer IV. Scale bar, 30 μm (F), 20 μm (K).

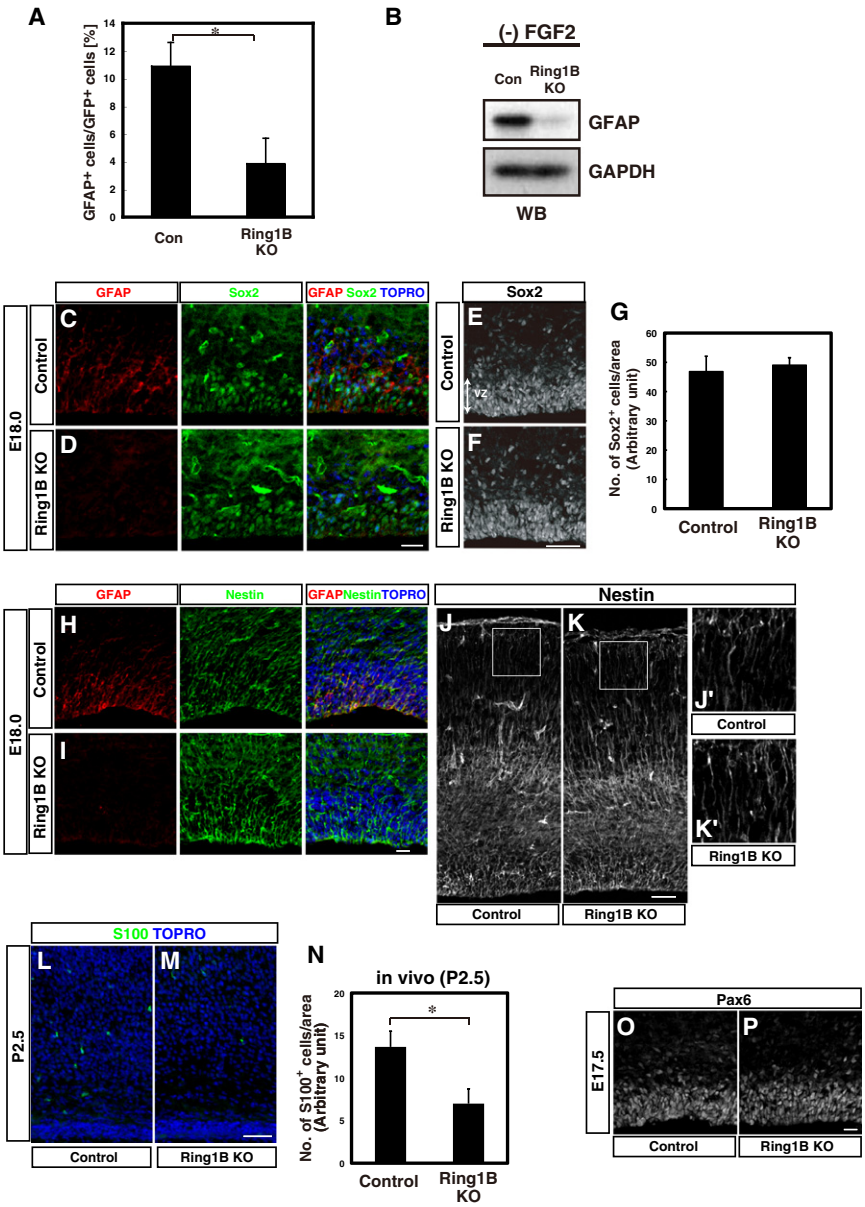

Figure 5. Ring1B/PRC1 Is Necessary for the Onset of Astrogenesis in the Neocortex

(A and B) E12.5 *Ring1B*$^{f/f}$;ERT2-Cre NPCs were cultured for 9 DIV and then treated with 4-OHT (KO) or EtOH (Con) for an additional 3 DIV. Cells were then plated and infected with a retrovirus encoding GFP in the presence of FGF2. After 2 days with (A) or 4 days without (B) FGF2, the percentages of GFAP$^+$ cells among GFP$^+$ cells (A) or the amounts of GFAP protein (B) were determined. Data are means + SEM of values from eight samples.

(C–P) Tamoxifen was introduced into *Ring1B*$^{f/f}$;NestinCreERT2 mice at E13.0 (C–K), E12.5 (O and P), or E14.5 (L–N), and the embryos were fixed at E18.0 (C–K), E17.5 (O and P), or P2.5 (L–N) and subjected to immunohistochemistry using the antibodies indicated. Nuclei were counterstained with Topro-3. Scale bars, (D, I, and P) 20 μm, (K and M) 50 μm, (F) 100 μm. (G) Quantification of Sox2$^+$ cells in the neocortical ventricular zone (VZ) at E18.0. (J' and K') Higher magnification of the insets in (J) and (K). (N) Quantification of S100$^+$ cells in the neocortex. Data are the mean + SEM of values for six areas of corresponding three sections each from control and KO mice (G) or five (control) or three (KO) areas of corresponding sections (N) analyzed.

in a clonal assay in the presence of S33Yβ-catenin (Figure 4D). These results indicate that PRC1/Ring1B instructs neuronal fate rather than promotes selective proliferation or survival of neuronal progenitors in the late stages of NPC culture.

We then tested whether PRC1/Ring1B indeed suppresses neurogenesis in vivo at late stages of neocortical development. To examine late stage phenotypes, we conditionally deleted the *Ring1B* gene in the central nervous system using mice harboring *Ring1B*$^{f/f}$ and an ERT2-Cre transgene under the control of the nestin enhancer (*Ring1B*$^{f/f}$;NestinERT2-Cre mouse). The major wave of neurogenesis is normally terminated perinatally. Birthdating studies have revealed that neocortical neurons can be labeled by BrdU at E18.5 but not at E19.0 when examined 20 days after BrdU injection (Levers et al., 2001). We confirmed that BrdU-labeled cells were hardly found in the upper layer of the neocortex at P6.5 when BrdU was injected into control mice at E19.0 (Figure 4E). However, when *Ring1B* was deleted by injecting tamoxifen intraperitoneally into pregnant mice at 13.5 dpc, the number of Cux1-positive late-born/upper-layer neurons in the cortical plate at P6.5 that had been labeled with BrdU at E19.0 was significantly greater than that in control siblings (Figures 4E–4G and S8). We indeed found that Ring1B deletion significantly increased Cux1-positive and Brn2-positive upper-layer neurons, visible as thicker (and more dense) upper cortical layers (Figures 4H–4L). These results demonstrate an in vivo role of *Ring1B* /PRC1 in the suppression of neurogenesis and termination of the neurogenic phase. An expansion of neuronal precursors might also contribute to the increased neuronal numbers in these mutant mice, although we could not directly address this possibility experimentally.

PRC1 Promotes the Onset of Gliogenesis in Neocortical Development

The next important question is whether PcG regulates the onset of gliogenesis (and thus fate conversion of NPCs) at late stages of development. Deletion of *Ring1B* from NPCs isolated from *Ring1B*$^{f/f}$;ERT2-Cre mice by 4-OHT treatment significantly reduced astrocyte differentiation induced by growth factor deprivation at the late stage (12 DIV) (Figure 5A). Inhibition of GFAP expression by *Ring1B* deletion at the late stage was

confirmed by western blot analysis (Figure 5B). Therefore, Ring1B/PRC1 appears to be necessary for the induction of astrocyte differentiation in the late stage in vitro.

We further examined astrogenesis in vivo. Whereas GFAP-positive cells could already be detected in the lateral VZ of control neocortex at E18.0, GFAP expression was barely detectable in the corresponding region of *Ring1B*-deficient mice (Figures 5C, 5D, 5H, and 5I). Similarly, the number of cells positive for another astrocytic marker S100β was also markedly reduced in the neocortex of *Ring1B*-deficient mice at P2.5 (Figures 5L–5N). Radial fibers of NPCs and the overall brain architecture appeared normal in these mice as visualized by immunohistochemistry using antibodies against Nestin (Figures 5H, 5I, and 5J–5K′). These results indicate that the PcG proteins are essential for promoting the onset of the astrocytic differentiation of NPCs during neocortical development.

Importantly, the numbers of cells positive for the NPC markers Sox2 or Pax6 were not reduced at E17.5 (Figures 5C–5G, 5O, and 5P), in fact, the number of Sox2-positive cells increased slightly at P3 following *Ring1B* deletion (Figure S6C). These results demonstrate that PRC1 inactivation does not lead to precocious differentiation and exhaustion of NPCs during late stages of neuronal development, supporting the notion that PRC1 contributes to the temporal switch in NPC differentiation potential.

In ES cells, *Ring1B* deletion resulted in derepression of developmental genes of various lineages (Figure 8A and (Endoh et al., 2008; van der Stoop et al., 2008)). In contrast, *Ring1B* deletion in the late stage (E18.5 + 4 DIV) of neocortical NPCs selectively derepressed genes associated with the neuronal lineage (Figure 8A and Table S1). This suggests a restricted/selective function for PRC1 in the late stage of neocortical development.

PRC2 Promotes Neurogenic-to-Gliogenic Fate Switching in Neocortical NPCs

Although PRC2 and PRC1 have been proposed to act together on chromatin silencing, it has also been suggested that these two complexes have distinct functions. Therefore, we examined whether PRC2 shares functions with PRC1 in the regulation of neocortical NPC fate. We first knocked down *Eed*, an essential component of PRC2 (Schwartz and Pirrotta, 2007) by introducing short hairpin RNA (shRNA) against *Eed* into NPCs by retroviral infection (see Experimental Procedures). *Eed* knockdown dramatically enhanced neuronal differentiation induced by the GSK3 inhibitor SB216763 in E11.5 + 9 DIV but not 3 DIV cultures, indicating that reduction of *Eed* overcame the suppression of neurogenesis in late-stage cultures (Figure 6A). When *Eed* was knocked down, SB216763 treatment also caused a reduction in the percentage of cells expressing the astrocyte marker GFAP among GFP-positive cells in E11.5 + 9 DIV culture (Figure 6B), suggesting that Eed confers gliogenic competence in late-stage cultures.

Two methyltransferases, Ezh1 and Ezh2, have been identified as PRC2 components that catalyze H3K27me3 (Cao and Zhang, 2004; Shen et al., 2008). We generated a mouse line in which the SET domain of *Ezh2* was flanked by loxP sequences, and crossed it with ERT2-Cre mice (Figures 7A and 7B). Treatment of neocortical NPCs isolated from the *Ezh2Δset*$^{f/f}$;ERT2-Cre

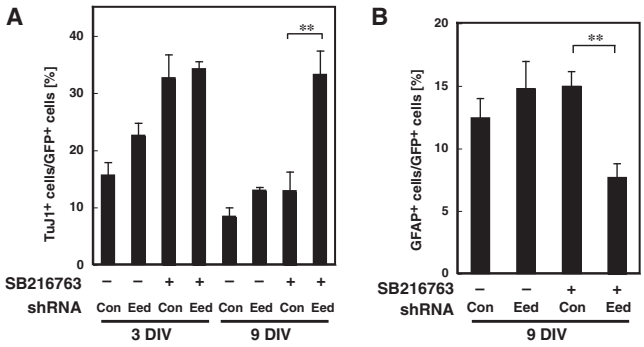

Figure 6. Eed/PRC2 Is Necessary for Suppression of Neurogenesis and Promotion of Astrogenesis

NPCs from E11.5 neocortex were cultured for 3 or 9 DIV and infected with a retrovirus encoding GFP with control shRNA (Control) or GFP together with shRNA for Eed. Cells were then treated with or without the GSK3 inhibitor SB216763 and cultured for 2 days without FGF2. The percentage of TuJ1$^+$ cells (A) or GFAP$^+$ cells (B) among GFP$^+$ cells was determined. Data are means + SEM of values from three samples.

mice at E12.5 with 4-OHT almost completely abolished expression of intact *Ezh2* mRNA (data not shown). The levels of H3K27me3 were also reduced by 4-OHT treatment in these cells (Figure 7C), suggesting that Ezh2 plays a major role in catalyzing H3K27me3 in neocortical NPCs. *Ezh2* deletion significantly increased the levels of *ngn1* mRNA, but not those of *ngn2* mRNA, in the absence of FGF2 (Figures 7D, S7A, and S7B). Furthermore, *Ezh2* gene deletion markedly enhanced neuronal differentiation induced either by FGF2 deprivation (Figure 7E) or by expression of S33Yβ-catenin (Figures 7F and 7G) at 9 DIV, whereas it suppressed astrocyte differentiation induced by S33Yβ-catenin (Figure 7H). This supports the notion that PRC2 restricts neurogenic competence in NPCs and triggers neurogenic-to-astrogenic fate switching. We further examined the role of Ezh2 in vivo by conditional deletion of the *Ezh2* gene in the central nervous system. When *Ezh2* was deleted in the *Ezh2Δset*$^{f/f}$;ERT2-Cre mice by introducing tamoxifen at E12.5, there were very little H3K27me3 signals in the ventricular zone cells of the neocortex at E17.5 (Figures 7I and 7J), again indicating that Ezh2 is responsible for this histone modification in these cells. Importantly, in these *Ezh2*-deficient mice, the reduction of Ngn1-positive cells in the late neurogenic phase such as E17.5 was significantly suppressed (Figures 7K–7M). Consistent with this finding, when *Ezh2* was deleted in the central nervous system in the *Ezh2Δset*$^{f/f}$;NestinERT2-Cre mice by introducing tamoxifen at E13.5 and E14.5, the number of S100β-positive cells was reduced in the neocortex at P1.5 (Figures 7P–7R). Taken together, these results support the notion that PRC2, as well as PRC1, contributes to suppression of Ngn1 and the transition of NPC fate from neurogenic to astrogenic during late stages of neocortical development.

DISCUSSION

One of the fundamental questions in understanding tissue development is how multipotent progenitors/tissue stem cells give

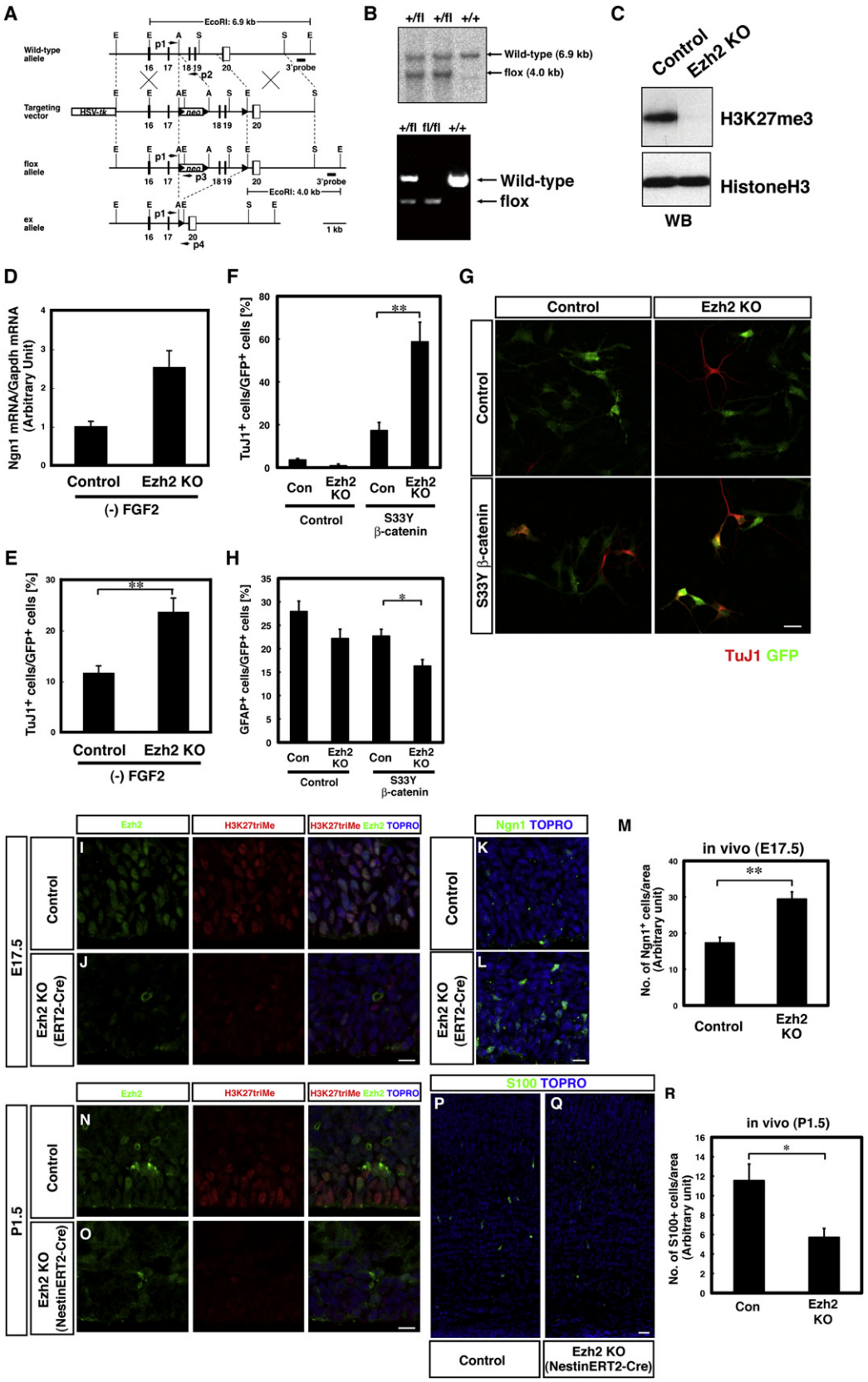
A
EcoRI: 6.9 kb
Wild-type allele
Targeting vector
HSV-tk
neo
flox allele
ex allele
3'probe
EcoRI: 4.0 kb
1 kb
B
+/fl +/fl +/+
Wild-type (6.9 kb)
flox (4.0 kb)
+/fl fl/fl +/+
Wild-type
flox
C
Control
Ezh2 KO
H3K27me3
HistoneH3
WB
D
Ngn1 mRNA/Gapdh mRNA (Arbitrary Unit)
Control
Ezh2 KO
(-) FGF2
F
TuJ1+ cells/GFP+ cells [%]
Con
Ezh2 KO
Control
S33Y β-catenin
G
Control
Ezh2 KO
S33Y β-catenin
TuJ1 GFP
E
TuJ1+ cells/GFP+ cells [%]
H
GFAP+ cells/GFP+ cells [%]
Ezh2
H3K27triMe
H3K27triMe Ezh2 TOPRO
Ngn1 TOPRO
E17.5
Control
Ezh2 KO (ERT2-Cre)
M
in vivo (E17.5)
No. of Ngn1+ cells/area (Arbitrary unit)
P1.5
Ezh2 KO (NestinERT2-Cre)
S100 TOPRO
R
in vivo (P1.5)
No. of S100+ cells/area (Arbitrary unit)

rise to various cell types in a defined order to achieve appropriate tissue organization. Neural stem cells (or NPCs) attract much attention since these cells give rise to neuronal and glial cell types in a temporally defined sequence in a developmental-stage-dependent manner with a striking precision. In this study, we have shown that a PcG-mediated epigenetic mechanism plays a pivotal role in driving the transition from the neurogenic phase to the astrogenic phase in NPCs during the mouse neocortical development. Deletion of *Ring1B* or *Ezh2*, as well as knockdown of Eed, prolonged the neurogenic phase and delayed the astrogenic phase in cultures of neocortical NPCs. Importantly, deletion of *Ring1B* did not reduce the numbers of Sox2- and Pax6-positive NPCs in the ventricular zone of the neocortex. Moreover, neuronal differentiation of cultured neocortical NPCs from *Ring1B*- or *Ezh2*-deficient embryos was still regulated normally and required differentiation conditions, such as expression of stabilized β-catenin or growth factor deprivation. These results indicate that PcG proteins regulate the differentiation capacity of NPCs without affecting the differentiation process per se.

During neocortical development, the neurogenic phase normally persists for a limited time period (about 11 cell cycles on average in the mouse neocortex [Takahashi et al., 1999]), and this restricted period may be a major parameter in determining the final number of neurons produced during development. Our results demonstrate that PcG proteins contribute to the termination of the neurogenic phase, which normally takes place between E18.5 and E19.0 in the neocortex (Levers et al., 2001). Indeed, birthdating analysis showed that cells labeled by BrdU at E19.0 still contributed to upper-layer neurons at P6.5 in *Ring1B*- or *Ezh2*-deficient mice but not in control mice. Interestingly, the excess neurons produced at around the end of neurogenic phase appear to be eliminated (probably by cell death [Verney et al., 2000]) later during postnatal development in both wild-type and *Ring1B*-deficient mice (data not shown), suggesting that these late-born excess neurons fail to integrate into the appropriate neuronal networks and therefore cannot be supported by activity/target-dependent survival signals. In other words, the correct timing of the end of neurogenesis might help avoid production of excess (unnecessary, undesirable) neurons.

The roles of PcG in ES cells strikingly differ from those in NPCs. Components of the PcG are known to localize and repress a variety of target genes and play an essential role in the maintenance of pluripotency of ES cells by suppressing differentiation into multiple lineages (Boyer et al., 2006; Endoh et al., 2008; Lee et al., 2006). A previous report has shown that different arrays of genes are labeled with H3K27me3 in ES cells and ES-derived neuronal progenitors (Mohn et al., 2008), suggesting that PcG targets are different between these cell types. Indeed, we found that *Ring1B* deletion in late-stage neocortical NPCs preferentially increases the expression of genes associated with neuronal differentiation/development over those associated with other lineages based on microarray analyses, whereas developmental genes in multiple lineages are derepressed by *Ring1B* deletion in ES cells.

The fate restriction of ES cells during differentiation is accompanied by diminished occupancy of H3K27me3 at specific "bivalent" gene promoters involved in the corresponding differentiation process (Mikkelsen et al., 2007), in contrast to the increased H3K27me3 at *ngn* loci during fate restriction of NPCs. Moreover, deletion of *Ring1B* or *Suz12* in ES cells results in the loss of neurogenic capacity (Pasini et al., 2007; van der Stoop et al., 2008), whereas deletion of *Ring1B* in the late NPCs extended neurogenic capacity. These observations further support the difference of PcG functions between these cell types. Thus, this study has unveiled an in vivo role of PcG, namely, temporal (stage-dependent) fate conversion of multipotent progenitors during development.

We found that PcG is responsible for *ngn1* suppression in late-stage NPCs. Since misexpression of *ngn1* extends neurogenesis in late-stage NPCs, it is clear that suppression of *ngn1* is a prerequisite for the neuronal-to-glial transition of NPC fate. Therefore, the suppression of *ngn1* by PcG may partly account for the PcG restriction of neurogenic potential and transition to gliogenesis in the neocortex. However, it is unclear whether PcG also regulates other genes with similar functions. *Ngn2* might be such a target, given that the level of H3K27me3 increases at the *ngn2* locus in the late stage of neocortical NPCs. However, *Ring1B* deletion by itself did not cause much increase in *ngn2* expression, suggesting that additional mechanisms might account for suppression of *ngn2* at late stages of neocortical development.

Besides *ngn1*, we did not find any other proneural genes that were greatly upregulated by *Ring1B* deletion in neocortical NPCs. For instance, there was no elevation in neurogenic genes expressed in the neocortex such as Pax6, Math1, and Mash1 (Britz et al., 2006; Guillemot, 2007; Schuurmans et al., 2004).

Figure 7. Ezh2/PRC2 Is Necessary for Suppression of Neurogenesis and Promotion of Astrogenesis

(A and B) Conditional disruption of the *Ezh2* locus. (A) Schematic representation of wild-type *Ezh2* allele, the targeting vector, and the resulting floxed and ex alleles. See the Supplemental Data for the full details (A). Southern blot analysis with EcoRI digestion (upper panel) and PCR analysis using genomic DNA (lower panel) from ES cells and tails, respectively (B).

(C–H) E12.5 *Ezh2Δset*$^{f/f}$;ERT2-Cre NPCs cultured for 12 DIV were treated as Figure 4 . Cell lysates were subjected to western blotting with antibodies indicated (C). After 3 hr of FGF2 deprivation, the amount of *ngn1* mRNA was determined (D). Cells were infected with a retrovirus encoding GFP and cultured without FGF2 for 2.5 days (E). Cells were infected with a retrovirus encoding GFP (control) or GFP together with S33Yβ-catenin in the presence of FGF2 (F–H). After 2.5 days, the percentages of TuJ1$^+$ cells (E–G) or those of GFAP$^+$ cells (H) among GFP$^+$ cells were determined. (G) Anti-GFP (green) and TuJ1 (red) immunofluorescence are shown for typical fields in control or S33Yβ-catenin expressing control or Ezh2 KO cells. Data are means + SEM of values from three samples.

(I–R) Tamoxifen was introduced into *Ezh2Δset*$^{f/f}$;ERT2-Cre mouse at E12.5 (I–M) or *Ezh2Δset*$^{f/f}$;NestinCreERT2 mouse at E13.5 and E14.5 (N–R). At E17.5 (I–L) or P1.5 (P–R), embryos were fixed and subjected to immunohistochemistry with antibodies indicated. (M) Quantification of Ngn1$^+$ cells at E17.5. (R) Quantification of S100$^+$ cells at P1.5. Data are the mean + SEM of values for 24 corresponding areas from three control mice or 32 corresponding areas from four KO mice (M) or 11 corresponding areas from three control mice or seven corresponding areas from two KO mice (R). Scale bars, (J, L, and O) 10 μm, (G and Q) 20 μm.

A

ESC

p value	GO
1.1E-13	cell adhesion
3.0E-13	pattern specification
4.4E-13	transmembrane receptor protein tyrosine kinase signaling pathway
3.8E-11	organ morphogenesis
2.5E-10	immune response
2.4E-08	inflammatory response
1.5E-07	phosphate transport
1.6E-07	skeletal development
8.5E-07	axon guidance
1.3E-06	eye development
2.2E-06	neuron differentiation
3.4E-06	proteolysis
6.4E-06	positive regulation of angiogenesis
1.0E-05	limb morphogenesis
2.2E-05	cell-cell signaling
2.2E-05	embryonic limb morphogenesis
2.3E-05	striated muscle contraction
2.4E-05	antigen processing and presentation of peptide antigen via MHC class I
2.6E-05	positive regulation of transcription from RNA polymerase II promoter
2.9E-05	neuron development
4.4E-05	defense response
7.2E-05	patterning of blood vessels
7.8E-05	G-protein coupled receptor protein signaling pathway

NPC

p value	GO
9.6E-10	ion transport
1.6E-08	synaptic transmission
2.6E-08	neuron differentiation
1.4E-07	development
5.8E-07	gamma-aminobutyric acid signaling pathway
6.2E-07	neurotransmitter secretion
1.2E-06	potassium ion transport
1.4E-06	pattern specification
1.4E-06	G-protein coupled receptor protein signaling pathway
1.5E-06	regulation of transcription
2.9E-06	signal transduction
2.9E-06	cell adhesion
1.3E-05	nervous system development
2.3E-05	brain development
2.6E-05	positive regulation of microtubule polymerization
6.2E-05	neuron migration
6.9E-05	positive regulation of transcription

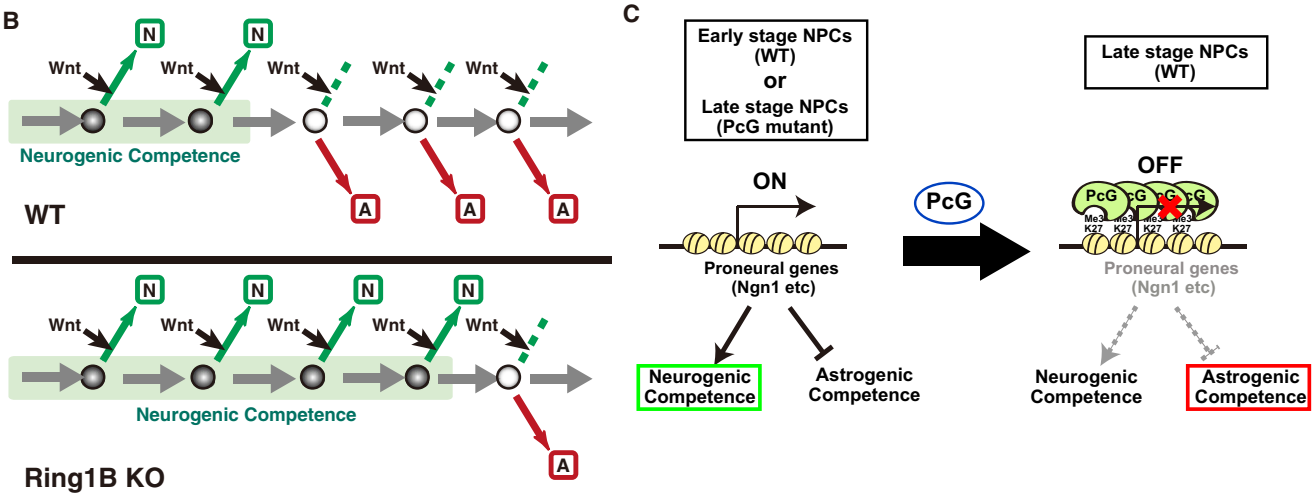

Figure 8. Ring1B/PRC1 Deletion in NPCs Derepresses Genes Associated with the Neuronal Lineage

(A) Gene ontology (GO) analysis of Ring1B/PRC1 target genes in ES cells and neocortical NPCs. NPCs isolated from the E18.5 *Ring1B*$^{f/f}$;ERT2-Cre mice were cultured for 1 DIV and cultured with 4-OHT (KO) or EtOH (Con) as a negative control for an additional 3 DIV. Then cells were plated and cultured 1 day followed by withdrawal of FGF2. After 2 hr, cells were harvested and subjected to microarray analysis. The significance (p value) of the enrichment is based on a hypergeometric distribution. All the significantly (p value < 10^{-5}) enriched terms classified in GO category Biological Process were indicated.

(B and C) Proposed model of the role of PcG proteins in the temporal fate regulation of NPCs. N, neuron; A, astrocyte.

Among the basic helix-loop-helix or homeodomain-containing transcription factors expressed in brain, *Dlx2* was significantly derepressed by *Ring1B* deletion (Table S1). Although Dlx2 can contribute to neurogenesis in the ventral telencephalon in some contexts (Brill et al., 2008; Lim et al., 2009), we do not think that this gene is responsible for the PcG suppression of neurogenesis in the neocortex, since Dlx2 is associated with differentiation of GABAergic interneurons rather than the glutamatergic neurons (Panganiban and Rubenstein, 2002) we observed in the *Ring1B*-deficient mice. Nonetheless, a recent report has shown that the chromatin remodeling factor Mll1 suppresses the accumulation of H3K27me3 at the *dlx2* locus and thus confers neurogenic potential in the adult neural stem cells (Lim et al., 2009). This implies a very interesting possibility that PcG participates in a common mechanism that suppresses neurogenic potential in both dorsal and ventral telencephalon in the late stages of development, and a small NPC population that escapes from this mechanism by Mll1 is selected to become

adult neural stem cells that continue to produce neurons for lifetime.

Although knockdown of *Bmi1*, a component of PRC1, resulted in NPC loss and brain size reduction in a previous study (Fasano et al., 2007), we did not observe these phenotypes in the *Ring1B*-deficient mouse, implicating that Bmi1 and Ring1B may form distinct complexes that exert different functions. These functions of Bmi1 may not be related to PRC2, since we found that brain size reduction was not seen in mice deficient for *Ezh2* in the central nervous system under the conditions corresponding to Figure 7, although H3K27me3 modification was barely seen in NPCs from these mice. Functional differences between Bmi1 and PRC2 have also been suggested in the hematopoietic system and tumors (Lessard et al., 1999; Pietersen et al., 2008). For example, Bmi1 deletion reduced the numbers of myeloid and preB cells, whereas Eed deletion increased these cell types (Lessard et al., 1999).

The levels of H3K27me3 gradually increase over time at the *ngn1* promoter, and it is plausible that, at a certain threshold, their chromatin state becomes inactivated by PRC1, resulting in the suppression of *ngn* expression and the transition of NPC fate. We propose that the developmental-stage-dependent accumulation of H3K27me3 at specific gene loci functions as a timer to drive cell fate switching. Exactly how this accumulation occurs is not clear at present but might involve either a global increase in PcG activity or local recruitment of PcG to the *ngn1* locus in late stages of neocortical NPCs. In either case, further analysis of this accumulation may shed light on the mechanism that underlies the developmental regulation of differentiation potential.

EXPERIMENTAL PROCEDURES

Generation of Mutant Mice and Animal Treatment

For conditional disruption of the *Ezh2* locus, see Supplemental Data. For conditional disruption of the *Ring1B* or *Ezh2* gene, the *Ring1B*$^{f/f}$ mouse (Cales et al., 2007; Endoh et al., 2008) or *Ezh2Δset*$^{f/f}$ mouse was crossed with either a ROSA26::
ERT2-Cre mouse (ERT2-Cre driven by the endogenous Rosa26 promoter) or a NestinERT2-Cre mouse (ERT2-Cre driven by the nestin enhancer) (Endoh et al., 2008; Imayoshi et al., 2006).

Tamoxifen (Sigma) was dissolved in corn oil (Nacalai) at a concentration of 10 mg/ml. Pregnant mice were injected intraperitoneally with 150 μl of tamoxifen solution for inducing ERT2-Cre activity.

All mice were maintained according to the protocol approved by the Animal Care and Use Committee of the University of Tokyo.

Expression Constructs and Antibodies

For expression constructs and the antibodies used in this study, see Supplemental Data.

Immunohistochemistry, Quantification, and Statistics

Immunohistochemistry was performed as previously described (Britz et al., 2006; Hirabayashi et al., 2004). Cells positive for the markers were counted in at least three 200 μm (or 90 μm in Figure 4L) wide bins spanning the primary sensory area and data are shown as the mean + SEM of values. Data for ChIP and mRNA quantification are the mean + SEM for three samples. Data for luciferase assay are the mean + SD of values from three samples. All data are representative of results obtained from at least three independent experiments. Statistical significance is determined by Student's t test.

Primary NPC Culture, Immunostaining, and Pharmacological Treatment

Primary NPCs were prepared from the dorsal cerebral cortex of ICR mouse embryos at E11.5 (E1 was defined as 12 hr after detection of the vaginal plug). Dissected cortices were transferred to artificial cerebrospinal fluid (aCSF: 124 mM NaCl, 5 mM KCl, 0.1 mM $CaCl_2$, 26 mM $NaHCO_3$, 1.3 mM $MgCl_2$, 10 mM glucose) containing 0.05% trypsin (Sigma) and incubated for 10 min on ice to remove overlying epidermal ectoderm. The cortices were then transferred to aCSF containing 0.1% trypsin, DNase I (0.1 mg/ml) (Roche), and hyaluronidase (0.67 mg/ml) (Sigma) and incubated at 37°C for 10 min. After the addition of an equal volume of aCSF containing trypsin inhibitor (0.7 mg/ml) (Sigma), the neuroepithelium was transferred to DMEM-F12 (1:1) and mechanically dissociated into single cells. The dissociated cells were cultured in DMEM-F12 (1:1) supplemented with B27 (Invitrogen), FGF2 (20 ng/ml) (R & D), and EGF (20 ng/ml) (Upstate Biotechnology). For retroviral infection, cells were mixed with recombinant viruses for 24 hr, washed with phosphate-buffered saline (PBS), and then incubated in the absence or presence of FGF2. For immunostaining, cells were fixed with 4% paraformaldehyde in PBS, permeabilized with 0.5% Triton X-100 for 30 min, incubated with primary antibodies for overnight and then with secondary antibodies for 30 min, and mounted in Mowiol (Calbiochem).

Valproic acid (VPA, Sigma) was dissolved in H_2O at a concentration of 1 M and added to culture medium at a final concentration of 1 μM. SB216763 (Tocris) was dissolved in DMSO at a concentration of 10 mM and added to culture medium at a final concentration of 12 μM. 4-hydroxytamoxifen (4-OHT, Sigma) was dissolved in EtOH at a concentration of 1 mM and added to culture medium at a final concentration of 125 nM.

Clonal Analysis

Clonal analysis was performed as previously described (Hirabayashi et al., 2004). NPCs (7.9×10^2 cells/mm^2) were plated on dishes coated with poly-D-lysine and infected with retroviruses encoding either GFP alone (control) or both GFP and S33Y β-catenin at a low titer (0.21 infected cells/mm^2).

RT-PCR

Total RNA was obtained from infected NPCs using TRIzol (Invitrogen) or RNAiso (Takara) following the instructions of the manufacturer. Reverse transcription (RT) was performed with 5 μg of total RNA, oligo $d(T)_{12-18}$ (Invitrogen) primers, and ReverTra Ace (TOYOBO). The resulting cDNA was subjected to real-time PCR in a Roche LightCycler with SYBR *Premix Ex Taq* (Takara). The abundance of target mRNAs was normalized relative to that of GAPDH mRNA. The primers were listed in Supplemental Data.

Chromatin Immunoprecipitation Assay

Primary NPCs were cultured in suspension for 0, 3, 6, 9, 12, or 15 days, after which neurospheres were collected and dissociated. The cells were suspended in lysis solution (1% SDS, 10 mM EDTA, 50 mM Tris-HCl [pH 8.1]) and sonicated to shear genomic chromatin into DNA fragments of ~0.5 to 10 kb. The lysate was incubated for 2 hr with Dynabeads Protein A (Invitrogen), after which the beads were removed and the lysate was incubated overnight at 4°C with antibodies. After the addition of protein A beads, the mixture was incubated with rotation for 1 hr. The beads were then isolated and washed consecutively with a low-salt solution (0.1% SDS, 1% Triton X-100, 2 mM EDTA, 20 mM Tris-HCl [pH 8.1], 150 mM NaCl), a high-salt solution (0.1% SDS, 1% Triton X-100, 2 mM EDTA, 20 mM Tris-HCl [pH 8.1], 500 mM NaCl), a LiCl solution (0.25 M LiCl, 1% NP-40, 1% sodium deoxycholate, 1 mM EDTA, 10 mM Tris-HCl [pH 8.1]), and twice with a Tris-EDTA solution (10 mM Tris-HCl [pH 8.0], 1 mM EDTA). Immune complexes were then eluted from the beads with a solution containing 10 mM dithiothreitol, 1% SDS, and 0.1 M $NaHCO_3$, after which NaCl was added to a final concentration of 0.2 M and the eluate was incubated at 65°C overnight to induce the dissociation of proteins from DNA. The proteins were eliminated by digestion with proteinase K at 45°C for 1 hr, and the DNA was purified with a QIAquick spin column (QIAGEN). The eluted DNA was subjected to real-time PCR in a Roche LightCycler with SYBR-green Realtime PCR Master Mix. The abundance of target genome DNA was normalized relative to that of input. The sense and antisense primers, respectively, are listed in Supplemental Data.

RNA Interference

The pSIREN-siLuc (control shRNA) and pSIREN-siEed (Eed shRNA) retroviral constructs were generated in accordance with the manufacturers' instructions (BD Biosciences and Clontech). The target sequence for the Eed shRNA was 5′-GCTTTACGGTTATGGAATATC-3′.

The reduction of Eed mRNA by introduction of Eed shRNA was ~50% in the experiments of Figure 6 as judged by quantitative RT-PCR. This reduction was considerably high, since the infection efficiency of shRNA-encoding retroviruses in Figure 4 was ~70%, as judged by GFP fluorescence.

Gene Ontology Analysis

We performed Gene Ontology analysis using Mouse430_2.na25 annotation data provided by Affymetrix. Observed signals were processed with quantile normalization and probes were collected whose log2 ratios of intensities to control were more than 0.5.

All GO terms in the annotation file were statistically evaluated using hypergeometric mean. Significantly (p value $< 10^{-5}$) enriched terms classified in GO category Biological Process were indicated in Figure 8A.

SUPPLEMENTAL DATA

Supplemental Data include Supplemental Experimental Procedures, eight figures, and one table and can be found with this article online at http://www.cell.com/neuron/supplemental/S0896-6273(09)00633-3.

ACKNOWLEDGMENTS

Nestin-CreERT2 mice were kindly provided by Dr. Ryoichiro Kageyama. We thank Drs J.A. Cooper, M.E. Greenberg, and M. Lamphier for critical reading and Dr M. Higuchi for technical assistance. This work was supported by Grant-in-Aid for Scientific Research (A) and on Priority Areas-Molecular Brain Science from the MEXT of Japan (20022010).

Accepted: August 20, 2009
Published: September 9, 2009

REFERENCES

Aulehla, A., Wehrle, C., Brand-Saberi, B., Kemler, R., Gossler, A., Kanzler, B., and Herrmann, B.G. (2003). Wnt3a plays a major role in the segmentation clock controlling somitogenesis. Dev. Cell *4*, 395–406.

Barnabe-Heider, F., Wasylnka, J.A., Fernandes, K.J., Porsche, C., Sendtner, M., Kaplan, D.R., and Miller, F.D. (2005). Evidence that embryonic neurons regulate the onset of cortical gliogenesis via cardiotrophin-1. Neuron *48*, 253–265.

Berger, S.L. (2002). Histone modifications in transcriptional regulation. Curr. Opin. Genet. Dev. *12*, 142–148.

Bonni, A., Sun, Y., Nadal-Vicens, M., Bhatt, A., Frank, D.A., Rozovsky, I., Stahl, N., Yancopoulos, G.D., and Greenberg, M.E. (1997). Regulation of gliogenesis in the central nervous system by the JAK-STAT signaling pathway. Science *278*, 477–483.

Boyer, L.A., Plath, K., Zeitlinger, J., Brambrink, T., Medeiros, L.A., Lee, T.I., Levine, S.S., Wernig, M., Tajonar, A., Ray, M.K., et al. (2006). Polycomb complexes repress developmental regulators in murine embryonic stem cells. Nature *441*, 349–353.

Brill, M.S., Snapyan, M., Wohlfrom, H., Ninkovic, J., Jawerka, M., Mastick, G.S., Ashery-Padan, R., Saghatelyan, A., Berninger, B., and Gotz, M. (2008). A dlx2- and pax6-dependent transcriptional code for periglomerular neuron specification in the adult olfactory bulb. J. Neurosci. *28*, 6439–6452.

Britz, O., Mattar, P., Nguyen, L., Langevin, L.M., Zimmer, C., Alam, S., Guillemot, F., and Schuurmans, C. (2006). A role for proneural genes in the maturation of cortical progenitor cells. Cereb. Cortex *16* (*Suppl 1*), i138–i151.

Cai, L., Morrow, E.M., and Cepko, C.L. (2000). Misexpression of basic helix-loop-helix genes in the murine cerebral cortex affects cell fate choices and neuronal survival. Development *127*, 3021–3030.

Cales, C., Roman-Trufero, M., Pavon, L., Serrano, I., Melgar, T., Endoh, M., Perez, C., Koseki, H., and Vidal, M. (2007). Inactivation of the Polycomb group protein Ring1B unveils an antiproliferative role in hematopoietic cell expansion and cooperation with tumorigenesis associated to Ink4a deletion. Mol. Cell Biol. *28*, 1018–1028.

Cao, R., and Zhang, Y. (2004). The functions of E(Z)/EZH2-mediated methylation of lysine 27 in histone H3. Curr. Opin. Genet. Dev. *14*, 155–164.

Clark, S.J., Harrison, J., Paul, C.L., and Frommer, M. (1994). High sensitivity mapping of methylated cytosines. Nucleic Acids Res. *22*, 2990–2997.

Cohen, P., and Goedert, M. (2004). GSK3 inhibitors: development and therapeutic potential. Nat. Rev. Drug Discov. *3*, 479–487.

de Napoles, M., Mermoud, J.E., Wakao, R., Tang, Y.A., Endoh, M., Appanah, R., Nesterova, T.B., Silva, J., Otte, A.P., Vidal, M., et al. (2004). Polycomb group proteins Ring1A/B link ubiquitylation of histone H2A to heritable gene silencing and X inactivation. Dev. Cell *7*, 663–676.

Desai, A.R., and McConnell, S.K. (2000). Progressive restriction in fate potential by neural progenitors during cerebral cortical development. Development *127*, 2863–2872.

Endoh, M., Endo, T.A., Endoh, T., Fujimura, Y., Ohara, O., Toyoda, T., Otte, A.P., Okano, M., Brockdorff, N., Vidal, M., and Koseki, H. (2008). Polycomb group proteins Ring1A/B are functionally linked to the core transcriptional regulatory circuitry to maintain ES cell identity. Development *135*, 1513–1524.

Fan, G., Martinowich, K., Chin, M.H., He, F., Fouse, S.D., Hutnick, L., Hattori, D., Ge, W., Shen, Y., Wu, H., et al. (2005). DNA methylation controls the timing of astrogliogenesis through regulation of JAK-STAT signaling. Development *132*, 3345–3356.

Fasano, C.A., Dimos, J.T., Ivanova, N.B., Lowry, N., Lemischka, I.R., and Temple, S. (2007). shRNA knockdown of Bmi-1 reveals a critical role for p21-Rb pathway in NSC self-renewal during development. Cell Stem Cell *1*, 87–99.

Gaiano, N., and Fishell, G. (2002). The role of notch in promoting glial and neural stem cell fates. Annu. Rev. Neurosci. *25*, 471–490.

Gottlicher, M., Minucci, S., Zhu, P., Kramer, O.H., Schimpf, A., Giavara, S., Sleeman, J.P., Lo Coco, F., Nervi, C., Pelicci, P.G., and Heinzel, T. (2001). Valproic acid defines a novel class of HDAC inhibitors inducing differentiation of transformed cells. EMBO J. *20*, 6969–6978.

Guillemot, F. (2007). Spatial and temporal specification of neural fates by transcription factor codes. Development *134*, 3771–3780.

He, F., Ge, W., Martinowich, K., Becker-Catania, S., Coskun, V., Zhu, W., Wu, H., Castro, D., Guillemot, F., Fan, G., et al. (2005). A positive autoregulatory loop of Jak-STAT signaling controls the onset of astrogliogenesis. Nat. Neurosci. *8*, 616–625.

Hirabayashi, Y., and Gotoh, Y. (2005). Stage-dependent fate determination of neural precursor cells in mouse forebrain. Neurosci. Res. *51*, 331–336.

Hirabayashi, Y., Itoh, Y., Tabata, H., Nakajima, K., Akiyama, T., Masuyama, N., and Gotoh, Y. (2004). The Wnt/beta-catenin pathway directs neuronal differentiation of cortical neural precursor cells. Development *131*, 2791–2801.

Imayoshi, I., Ohtsuka, T., Metzger, D., Chambon, P., and Kageyama, R. (2006). Temporal regulation of Cre recombinase activity in neural stem cells. Genesis *44*, 233–238.

Israsena, N., Hu, M., Fu, W., Kan, L., and Kessler, J.A. (2004). The presence of FGF2 signaling determines whether beta-catenin exerts effects on proliferation or neuronal differentiation of neural stem cells. Dev. Biol. *268*, 220–231.

Johe, K.K., Hazel, T.G., Muller, T., Dugich-Djordjevic, M.M., and McKay, R.D. (1996). Single factors direct the differentiation of stem cells from the fetal and adult central nervous system. Genes Dev. *10*, 3129–3140.

Kamakura, S., Oishi, K., Yoshimatsu, T., Nakafuku, M., Masuyama, N., and Gotoh, Y. (2004). Hes binding to STAT3 mediates crosstalk between Notch and JAK-STAT signalling. Nat. Cell Biol. *6*, 547–554.

Kaykas, A., Yang-Snyder, J., Heroux, M., Shah, K.V., Bouvier, M., and Moon, R.T. (2004). Mutant Frizzled 4 associated with vitreoretinopathy traps wild-type Frizzled in the endoplasmic reticulum by oligomerization. Nat. Cell Biol. *6*, 52–58.

Korinek, V., Barker, N., Morin, P.J., van Wichen, D., de Weger, R., Kinzler, K.W., Vogelstein, B., and Clevers, H. (1997). Constitutive transcriptional activation by a beta-catenin-Tcf complex in APC−/− colon carcinoma. Science *275*, 1784–1787.

Lee, T.I., Jenner, R.G., Boyer, L.A., Guenther, M.G., Levine, S.S., Kumar, R.M., Chevalier, B., Johnstone, S.E., Cole, M.F., Isono, K., et al. (2006). Control of developmental regulators by Polycomb in human embryonic stem cells. Cell *125*, 301–313.

Lessard, J., Schumacher, A., Thorsteinsdottir, U., van Lohuizen, M., Magnuson, T., and Sauvageau, G. (1999). Functional antagonism of the Polycomb-Group genes eed and Bmi1 in hemopoietic cell proliferation. Genes Dev. *13*, 2691–2703.

Levers, T.E., Edgar, J.M., and Price, D.J. (2001). The fates of cells generated at the end of neurogenesis in developing mouse cortex. J. Neurobiol. *48*, 265–277.

Lim, D.A., Huang, Y.C., Swigut, T., Mirick, A.L., Garcia-Verdugo, J.M., Wysocka, J., Ernst, P., and Alvarez-Buylla, A. (2009). Chromatin remodelling factor Mll1 is essential for neurogenesis from postnatal neural stem cells. Nature *458*, 529–533.

Mikkelsen, T.S., Ku, M., Jaffe, D.B., Issac, B., Lieberman, E., Giannoukos, G., Alvarez, P., Brockman, W., Kim, T.K., Koche, R.P., et al. (2007). Genome-wide maps of chromatin state in pluripotent and lineage-committed cells. Nature *448*, 553–560.

Miller, F.D., and Gauthier, A.S. (2007). Timing is everything: making neurons versus glia in the developing cortex. Neuron *54*, 357–369.

Mohn, F., Weber, M., Rebhan, M., Roloff, T.C., Richter, J., Stadler, M.B., Bibel, M., and Schubeler, D. (2008). Lineage-specific polycomb targets and de novo DNA methylation define restriction and potential of neuronal progenitors. Mol. Cell *30*, 755–766.

Molne, M., Studer, L., Tabar, V., Ting, Y.T., Eiden, M.V., and McKay, R.D. (2000). Early cortical precursors do not undergo LIF-mediated astrocytic differentiation. J. Neurosci. Res. *59*, 301–311.

Naka, H., Nakamura, S., Shimazaki, T., and Okano, H. (2008). Requirement for COUP-TFI and II in the temporal specification of neural stem cells in CNS development. Nat. Neurosci. *11*, 1014–1023.

Nakashima, K., Yanagisawa, M., Arakawa, H., Kimura, N., Hisatsune, T., Kawabata, M., Miyazono, K., and Taga, T. (1999). Synergistic signaling in fetal brain by STAT3-Smad1 complex bridged by p300. Science *284*, 479–482.

Nieto, M., Schuurmans, C., Britz, O., and Guillemot, F. (2001). Neural bHLH genes control the neuronal versus glial fate decision in cortical progenitors. Neuron *29*, 401–413.

Nieto, M., Monuki, E.S., Tang, H., Imitola, J., Haubst, N., Khoury, S.J., Cunningham, J., Gotz, M., and Walsh, C.A. (2004). Expression of Cux-1 and Cux-2 in the subventricular zone and upper layers II-IV of the cerebral cortex. J. Comp. Neurol. *479*, 168–180.

Panganiban, G., and Rubenstein, J.L. (2002). Developmental functions of the Distal-less/Dlx homeobox genes. Development *129*, 4371–4386.

Pasini, D., Bracken, A.P., Hansen, J.B., Capillo, M., and Helin, K. (2007). The polycomb group protein Suz12 is required for embryonic stem cell differentiation. Mol. Cell. Biol. *27*, 3769–3779.

Pietersen, A.M., Horlings, H.M., Hauptmann, M., Langerod, A., Ajouaou, A., Cornelissen-Steijger, P., Wessels, L.F., Jonkers, J., van de Vijver, M.J., and van Lohuizen, M. (2008). EZH2 and BMI1 inversely correlate with prognosis and TP53 mutation in breast cancer. Breast Cancer Res. *10*, R109.

Qian, X., Shen, Q., Goderie, S.K., He, W., Capela, A., Davis, A.A., and Temple, S. (2000). Timing of CNS cell generation: a programmed sequence of neuron and glial cell production from isolated murine cortical stem cells. Neuron *28*, 69–80.

Rajan, P., and McKay, R.D. (1998). Multiple routes to astrocytic differentiation in the CNS. J. Neurosci. *18*, 3620–3629.

Sardi, S.P., Murtie, J., Koirala, S., Patten, B.A., and Corfas, G. (2006). Presenilin-dependent ErbB4 nuclear signaling regulates the timing of astrogenesis in the developing brain. Cell *127*, 185–197.

Schuurmans, C., Armant, O., Nieto, M., Stenman, J.M., Britz, O., Klenin, N., Brown, C., Langevin, L.M., Seibt, J., Tang, H., et al. (2004). Sequential phases of cortical specification involve Neurogenin-dependent and -independent pathways. EMBO J. *23*, 2892–2902.

Schwartz, Y.B., and Pirrotta, V. (2007). Polycomb silencing mechanisms and the management of genomic programmes. Nat. Rev. Genet. *8*, 9–22.

Shen, X., Liu, Y., Hsu, Y.J., Fujiwara, Y., Kim, J., Mao, X., Yuan, G.C., and Orkin, S.H. (2008). EZH1 mediates methylation on histone H3 lysine 27 and complements EZH2 in maintaining stem cell identity and executing pluripotency. Mol. Cell *32*, 491–502.

Shimogori, T., VanSant, J., Paik, E., and Grove, E.A. (2004). Members of the Wnt, Fz, and Frp gene families expressed in postnatal mouse cerebral cortex. J. Comp. Neurol. *473*, 496–510.

Song, M.R., and Ghosh, A. (2004). FGF2-induced chromatin remodeling regulates CNTF-mediated gene expression and astrocyte differentiation. Nat. Neurosci. *7*, 229–235.

Spivakov, M., and Fisher, A.G. (2007). Epigenetic signatures of stem-cell identity. Nat. Rev. Genet. *8*, 263–271.

Sun, Y., Nadal-Vicens, M., Misono, S., Lin, M.Z., Zubiaga, A., Hua, X., Fan, G., and Greenberg, M.E. (2001). Neurogenin promotes neurogenesis and inhibits glial differentiation by independent mechanisms. Cell *104*, 365–376.

Takahashi, T., Goto, T., Miyama, S., Nowakowski, R.S., and Caviness, V.S., Jr. (1999). Sequence of neuron origin and neocortical laminar fate: relation to cell cycle of origin in the developing murine cerebral wall. J. Neurosci. *19*, 10357–10371.

Takizawa, T., Nakashima, K., Namihira, M., Ochiai, W., Uemura, A., Yanagisawa, M., Fujita, N., Nakao, M., and Taga, T. (2001). DNA methylation is a critical cell-intrinsic determinant of astrocyte differentiation in the fetal brain. Dev. Cell *1*, 749–758.

Tomita, K., Moriyoshi, K., Nakanishi, S., Guillemot, F., and Kageyama, R. (2000). Mammalian achaete-scute and atonal homologs regulate neuronal versus glial fate determination in the central nervous system. EMBO J. *19*, 5460–5472.

Valk-Lingbeek, M.E., Bruggeman, S.W., and van Lohuizen, M. (2004). Stem cells and cancer; the polycomb connection. Cell *118*, 409–418.

van der Stoop, P., Boutsma, E.A., Hulsman, D., Noback, S., Heimerikx, M., Kerkhoven, R.M., Voncken, J.W., Wessels, L.F., and van Lohuizen, M. (2008). Ubiquitin E3 ligase Ring1b/Rnf2 of polycomb repressive complex 1 contributes to stable maintenance of mouse embryonic stem cells. PLoS ONE *3*, e2235.

Verney, C., Takahashi, T., Bhide, P.G., Nowakowski, R.S., and Caviness, V.S., Jr. (2000). Independent controls for neocortical neuron production and histogenetic cell death. Dev. Neurosci. *22*, 125–138.

Voncken, J.W., Roelen, B.A., Roefs, M., de Vries, S., Verhoeven, E., Marino, S., Deschamps, J., and van Lohuizen, M. (2003). Rnf2 (Ring1b) deficiency causes gastrulation arrest and cell cycle inhibition. Proc. Natl. Acad. Sci. USA *100*, 2468–2473.

Zhou, C.J., Borello, U., Rubenstein, J.L., and Pleasure, S.J. (2006). Neuronal production and precursor proliferation defects in the neocortex of mice with loss of function in the canonical Wnt signaling pathway. Neuroscience *142*, 1119–1131.